ISSN 1063-7745, Crystallography Reports, 2022, Vol. 67, No. 6, pp. 826–832. © Pleiades Publishing, Inc., 2022.
Russian Text © The Author(s), 2022, published in Kristallografiya, 2022, Vol. 67, No. 6, pp. 892–899.

DIFFRACTION AND SCATTERING OF IONIZING RADIATIONS

X-Ray Phase-Contrast Microscope: Theory and Computer Experiment

V. G. Kohn[a,b,*]

[a] *National Research Centre "Kurchatov Institute," Moscow, 123182 Russia*
[b] *Shubnikov Institute of Crystallography, Federal Scientific Research Centre "Crystallography and Photonics," Russian Academy of Sciences, Moscow, 119333 Russia*
**e-mail: kohnvict@yandex.ru*

Received January 29, 2022; revised January 29, 2022; accepted February 26, 2022

Abstract—A new method of X-ray microscopy using synchrotron radiation is theoretically analyzed. The method is based on the concepts of near-field phase contrast and nanofocusing using a planar compound refractive lens, which forms a secondary source with a small transverse size at a short distance from the sample. A computer experiment on imaging a two-dimensional photonic crystal with a period of 0.5 μm has been carried out. A universal program has been developed for carrying out computer experiments in the field of coherent X-ray optics. It is shown that the method proposed is characterized by high resolution, locality, and large luminosity; it is also weakly sensitive to the transverse size of a real synchrotron radiation source. The experimental setup may be rather compact and provide image magnification by a factor of more than 100.

DOI: 10.1134/S106377452206013X

INTRODUCTION

X-ray coherent optics has been widely used in scientific research since the middle of the 1990s, after the advent of third-generation synchrotron radiation (SR) sources; the first of such sources was the European Synchrotron Radiation Facility in Grenoble (France). Among the methods developed for the last 25 years, we should note the phase-contrast imaging of microscopic objects [1] and the SR beam focusing by compound refractive lenses (CRLs) [2].

For a hundred years after the discovery of X rays, imaging methods based on absorption of radiation by large objects without any significant refraction (i.e., change in the beam path) have been used in medicine and diagnostics of materials. The absorption contrast of small (less than 50 μm) objects consisting of light atoms is very weak. Using coherent radiation, one can record the contrast arising as a result of inhomogeneous refraction of rays in an object by measuring the SR intensity at some distance from the object. A strong contrast can be obtained at a fast change in the wave phase by only $\pi/4 = 0.785$. For example, in silicon this phase shift at a photon energy $E = 12.4$ keV is implemented on a thickness of 4 μm along the SR beam direction. A weak contrast can be obtained at thicknesses smaller than 1 μm.

The conventional phase-contrast method uses a wide SR beam, due to which a large crystal volume can be exposed. This is convenient, for example, when imaging microvoids in the bulk of silicon carbide crystal [3], when the object location in the sample is unknown beforehand. It follows from the theory that the diffraction of radiation from objects with a limited cross section (having a size D) yields radically different images, depending on the distance z_1 between the object and detector. The first Fresnel zone diameter depends on distance: $D_f = 2(\lambda z_1)^{1/2}$. From here on, $\lambda = hc/E$ is the SR wavelength after the transmission through the monochromator, h is Planck's constant, and c is the speed of light.

If $D \gg D_f$ (near field), the intensity changes only on the edges of the object, and its transverse size can be determined directly. If $D \ll D_f$ (far field), the radiation intensity recorded by the detector is the squared modulus of the function that is a Fourier transform of the radiation wave function directly after the object, changed additionally during the interference of the radiation scattered by the object and the radiation that by-passed the object. The intermediate range of distances is assigned to Fresnel diffraction, which has a more complex character.

Far field is considered in coherent diffraction imaging [4]. A narrow beam (limited by a slit) is used to suppress the interference and improve the coherence. Obviously, near field is most preferred for direct determination of the transverse sizes of microscopic objects. However, there are two problems to solve.

First, the distance at which the near-field condition is satisfied is fairly small; it may be on the order of few tenths of a millimeter. Second, the microscopic

object size is so small that it cannot be measured by a detector even with a resolution highest to date: ~0.5 μm. Hence, the image must be magnified. An analog of the focusing lenses used in visible light optics is X-ray CRLs, based on which a standard microscope can be designed [5]. The operation of this microscope is based on the lens formula

$$z_0^{-1} + z_1^{-1} = z_f^{-1},$$

where z_0 is the distance between the CRL and the point at which the SR intensity is "imaged," z_1 is the distance between the CRL and the detector (mounted after the CRL), and z_f is the CRL focal length. The SR intensity is generally "imaged" at a small distance after the object but before the CRL. The microscope can magnify any nonuniform intensity distribution.

An advantage of the above-described method is that an image is obtained directly and with a high resolution, which is determined by only the SR beam size at the CRL focus. The magnification factor, i.e., the ratio of the image size to the object size, is $M = z_1/z_0$. With allowance for the fact that z_0 should exceed z_f and that the CRL focal length is not very small, this scheme has a large longitudinal size.

In particular, the following values were used in [5]: $z_0 = 0.25$ m and $z_1 = 6$ m. A two-dimensional image of a photonic crystal with a period of 300 nm was obtained. As was theoretically shown later in [6, 7], the phase-contrast image of a large photonic crystal retains its periodicity, but the image itself changes very rapidly with an increase in distance after the object, and even the Talbot effect [8] is observed at a relatively short distance.

In this paper, we report the results of a theoretical analysis of another microscope scheme, which is much simpler and more compact than the scheme based on the lens formula. A necessary condition is the use of a nanofocusing CRL; i.e., the beam must have minimally possible sizes in the focus. Currently such lenses are fabricated on the silicon surface by microstructuring methods (see, e.g., [9–11]). They focus an SR beam only along one direction and are referred to as planar lenses. The new microscope uses the conventional scheme of near-field phase contrast, but in the flip form. The source and sample are spaced by a small distance z_0, and the structure of the image obtained barely depends on the distance z_1 to the detector (mounted after the sample). An important advantage of this scheme is that the image size rapidly increases with an increase in z_1.

These conditions cannot be provided using a real SR source. Therefore, it is proposed to use a secondary source that is formed at the CRL focus. The resolution of this scheme depends on the SR beam size at the CRL focus and on the angular divergence of SR beam after focusing.

FUNDAMENTALS OF THE THEORY AND NUMERICAL COMPUTATION PARAMETERS

To illustrate the concept of the proposed method, we will consider the well-known phase contrast theory. Coherent SR is emitted by individual electrons on an orbit, but the radiation from different electrons is incoherent. Since planar CRLs focus radiation only along the x axis, we will consider the (x, z) plane. The point source coordinate will be denoted as x_s. The SR wave function, i.e., the electric field strength after passing through the monochromator, will be presented as a product of fast and slow functions,

$$E(x, x_s, t) = \exp(ikz - i\omega t)A(x, x_s, \omega), \quad (1)$$

where t is time, $k = 2\pi/\lambda$, and $\omega = c/k$; the slow function has the form

$$A(x, x_s) = \int dx_0 P(x - x_0, z_1)T(x_0)P(x_0 - x_s, z_0). \quad (2)$$

In formula (2) z_0 and z_1 are, respectively, the source–object and object–detector distances. The Fresnel propagator

$$P(x, z) = (i\lambda z)^{-1/2} \exp(i\pi x^2/\lambda z) \quad (3)$$

makes it possible to calculate the SR beam propagation in empty space. It is the transverse part of spherical wave in the paraxial approximation. A microscopic object is described by the transmission function

$$T(x) = \exp(-ik[\delta - i\beta]t_0(x)), \quad (4)$$

where $\delta - i\beta = 1 - n$, n is the complex refractive index of SR in the material of microscopic object, and $t_0(x)$ is the profile of microscopic object thickness along the z axis at a specified coordinate x.

Formula (2) has a clear physical meaning. Radiation emitted at the point x_s passes the distance z_0 and then is transmitted through the object. The passage of the distance z_1 to the detector is taken into account by convolution of the Fresnel propagator and wave function according to the Huygens–Fresnel principle. Using mathematical calculations and the properties of Fresnel propagator (3), one can transform Eq. (2) as follows:

$$A(x, x_s) = P(x - x_s, z_t)a_i(x_i, z_i), \quad (5)$$

$$a_i(x_i, z_i) = \int dx_0 P(x_i - x_0, z_i)T(x_0), \quad (6)$$

$$\begin{aligned} z_t &= z_0 + z_1, \quad z_i = z_0 z_1/z_t, \\ x_i &= (z_0/z_t)[x + x_s(z_1/z_0)]. \end{aligned} \quad (7)$$

The first factor in (5) does not affect the intensity distribution and only scales it inversely proportional to the total distance z_t, whereas the second factor depends on the transverse coordinate and distance in the intrinsic coordinate system of the image.

Under conventional experimental conditions the inequality $z_0 \gg z_1$ is satisfied on the SR source. Here,

z_i differs very little from z_1, being only somewhat smaller. The near-field condition can be provided by decreasing the distance z_1. In this case the coordinate x_i differs very little from the real coordinate x, and the image is not magnified. As was noted above, these conditions are not suitable for imaging microscopic objects. A more attractive condition is the inverse one: $z_0 \ll z_1$. In this case z_i is almost equal to z_0, and $x = (z_t/z_0)x_i$ if $x_s = 0$. In other words, the near-field condition is independent of z_1. Therefore, the image is approximately retained with an increase in the distance between the object and detector, whereas its size is proportional to z_1, and a rather high magnification can be achieved.

The problem is that a real source cannot be approached closely to the sample. Moreover, the sizes of its projection will also be significantly increased, which will spoil completely the image quality. This problem can be solved using a nanofocusing CRL. To this end, another element must be placed before the sample in the conventional phase-contrast scheme. An analytical theory of focusing SR using a nanofocusing CRL was developed in [12, 13] for the case where the effective CRL aperture is twice as small as the real aperture. An algorithm for taking into account the real CRL aperture for hard radiation (a case where the aforementioned condition is invalid) was developed recently in [14, 15].

It is known that the theory of coherent X-ray optics based on the Maxwell equations and the quantum theory of interaction of radiation with material describes experimental results with a fairly high accuracy, provided that all parameters of the experiment and sample are exactly known (see, e.g., [16]). If some parameter is not exactly known, it can be determined by comparing the experiment with calculation (see, e.g., [17]). To carry out computer experiments in the field of coherent X-ray optics, the author wrote a universal computer program XRWP1 on his own language ACL; this program is run by the interpreter vkACL.jar written on Java. The interpreter and description of the language can be freely obtained on the Internet [18].

To illustrate the possibilities of the new phase-contrast method, the following parameters were chosen for the computer experiment: SR photon energy $E =$ 25 keV and the distance from the SR source to CRL is $z_s = 50$ m; the CRL parameters were taken from the real experiment [11]: aperture $A = 50$ μm, the radius of parabolic surface curvature is $R = 6.25$ μm, the length of one biconcave element is $p = 102$ μm, and the total number of CRL elements is 150. Using the on-line-program [19], one can easily find that the focal length of this CRL is $z_f = 2.1664$ cm, whereas the CRL length is $L = 1.53$ cm. The CRL effective aperture is $A_e = 18$ μm; this value satisfies the condition $A_e < A/2$, under which the real aperture does not affect the result.

The beam size (half-width of the intensity curve) at the focus (w_b) for a point source (diffraction limit), with the aperture disregarded [19], is 39 nm; a more accurate calculation using the XRWP1 program (with allowance for the aperture) yields 40 nm. To implement the near-field condition, one must approach the sample to the CRL focus as close as possible. However, a problem of finite angular divergence of the SR beam after focusing arises in this case. The theory says that, under the aforementioned conditions, the intensity profile at the focus is Gaussian and the phase is zero. The angular divergence of the beam can be calculated by the Fourier transform method. This beam parameter is completely determined by the beam size at the focus, is described by a Gaussian, and its half-width is

$$w_a = (2\ln 2/\pi)(\lambda/w_b) = 0.4413(\lambda/w_b). \quad (8)$$

For the aforementioned parameters ($w_b = 40$ nm, $\lambda =$ 0.0248 nm), expression (8) yields $w_a = 2.74 \times 10^{-4}$ rad.

The sample is shown in Fig. 1. It is a fragment of a two-dimensional photonic crystal in the form of a square lattice of cylinders with a period of 0.5 μm. The cylinder diameter is 0.3 μm. The fragment has 11 and 30 periods in the transverse and longitudinal directions, respectively. The longitudinal sample size is 15 μm. The beam size at a distance of $z_0 = 0.4$ cm from the lens focus is $w_a z_0 = 1.1$ μm. However, the half-width of the wave function modulus is 1.5 times larger; therefore, the SR beam illuminates three periods. This situation resembles that arising in the coherent diffraction imaging method. A narrow beam is an advantage for photonic crystals, because it increases the locality of the method. The entire crystal can be analyzed in the transverse direction by scanning the sample under a beam. Other (larger) samples can also be studied in this way.

The diameter of the first Fresnel zone for the aforementioned distance is $2(\lambda z_0)^{1/2} = 0.63$ μm; i.e., the near-field condition is now invalid. Nevertheless, the crystal period can still be determined with a relatively high accuracy. The influence of the beam size at the focus on the method resolution cannot be estimated using simple formulas. However, a computational experiment provides reliable results. A complete schematic of this experiment with the aforementioned distances is shown in Fig. 2.

This computational experiment is performed successively. First, the wave function before the CRL is determined in the form of a spherical wave in the paraxial approximation. Then its transmission through the CRL is calculated. Different methods serve for this purpose [14, 15], each of which uses the Fourier transform. The fast Fourier transform [20] is calculated on a grid containing $N = 2^k$ (k is an integer) points with a constant spacing. The grid spacing and number k are chosen such as to obtain a maximally exact result with necessary image detalization.

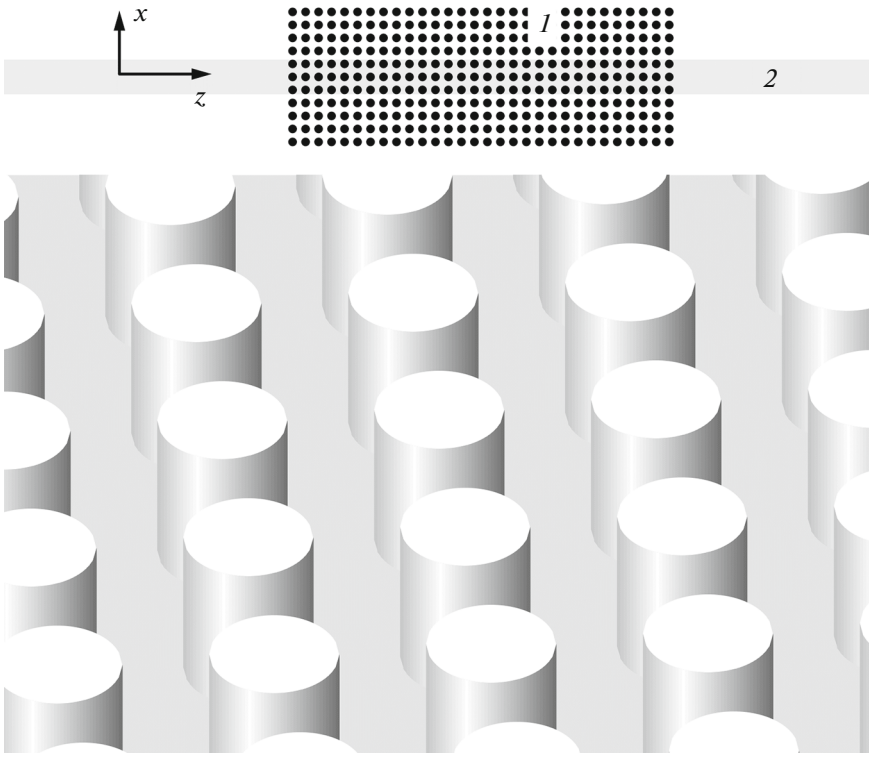

Fig. 1. Sample for the computer experiment as a part of a two-dimensional photonic crystal: (*1*) total number of cylinders and (*2*) narrow SR beam. A 3D image of photonic crystal is shown in the bottom.

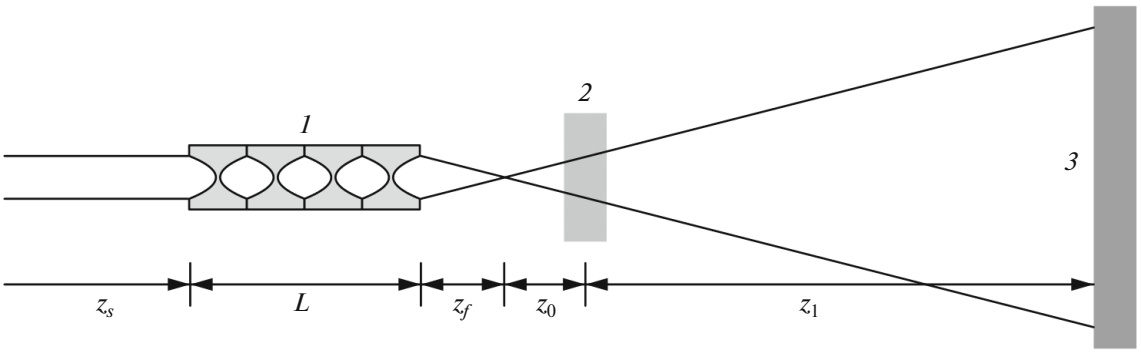

Fig. 2. General scheme of the computer experiment: (*1*) compound refractive lens, (*2*) sample, and (*3*) detector.

Then the wave function of the SR passing through empty space is calculated, and the fast Fourier transform method is applied again. The transmission of SR through the object is taken into account by multiplying by the transmission function (4), after which the transmission through empty space is taken into consideration again. This modular principle makes it possible to simulate experimental schemes of any complexity. If possible, all calculations are made on the same system of points. However, in exceptional cases the system of points can be changed, and one can pass from one system to another either interpolating the wave function or calculating the SR transmission through the object. All results were obtained using the same system of points with a step of 4 nm and a number of points equal to 2^{16}.

RESULTS AND DISCUSSION

The experimental scheme (Fig. 2) can be used in both near-field versions, i.e., when $z_0 > z_1$ and when $z_1 > z_0$. Let us consider the conventional scheme, i.e., the first version. Figure 3 shows four intensity distribution plots after the transmission through the model object (Fig. 1). The distance from the secondary source to the object is $z_0 = 10$ cm. The transverse beam

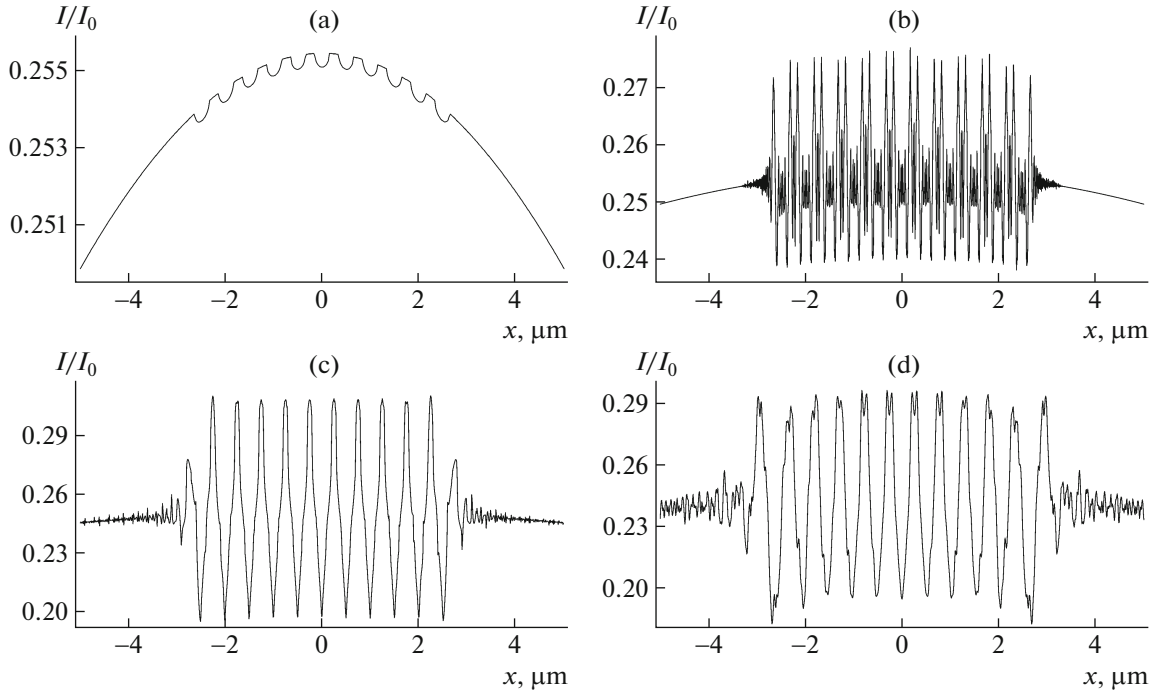

Fig. 3. Phase-contrast images of the photonic crystal at $z_0 = 10$ cm and z_1: (a) 0, (b) 0.01, (c) 0.1, and (d) 0.4 cm. Intensity I_0 refers to the beginning of CRL.

size is sufficiently large in this case, and the beam illuminates the entire piece of photonic crystal, consisting of 11 periods 5.5 μm in size. Note that all the distances considered in this figure cannot yet be implemented in a real experiment. However, everything is possible in a computer experiment.

Figure 3a shows the intensity distribution directly after the object ($z_1 = 0$). One can see that each cylinder absorbs radiation very weakly, and the absorption is maximum for the ray passing through the cylinder center. The relative contrast is 0.002. To distinguish it beyond the shot noise, more than 10^6 photons must be registered by the detector.

In Fig. 3b the distance $z_1 = 0.01$ cm. A fairly strong phase contrast arises on this negligibly small distance. The relative contrast is somewhat larger than 0.1. This is larger by a factor of 50 than in the previous case. Cylinders are known to give intensity interference peaks on edges (see, e.g., [17]). The distance between the peaks from one cylinder is larger than 0.3 μm; it is also larger than the distance between the peaks from two neighboring cylinders, which is smaller than 0.2 μm. In other words, the peak structure allows one to decipher the structure of the photonic crystal itself directly, without mathematical processing.

In Fig. 3c $z_1 = 0.1$ cm. One can see that the image structure is now much simpler, although the contrast is as high as it was. Similar peaks from neighboring cylinders merged into one peak. However, the photonic crystal period can still be seen well in the image, and it can be measured directly in the presence of a detector with such a high resolution. In Fig. 3d the distance $z_1 = 0.4$ cm. The image changed its structure again. It can be seen that the periods at edges are significantly distorted by the edge effect. In the central part the period is still observed well. It could also be measured, but the absence of image magnification does not allow one to do this.

Let us now analyze the results obtained in the new scheme. Now it is quite possible to approach the sample to the secondary source at an arbitrary small distance, because the CRL focal length $z_f = 2.1664$ cm, and this distance is macroscopic. However, the problem is that the beam is too narrow in this case. An intermediate version with $z_0 = 0.4$ cm was chosen. As was shown above, the photonic crystal period is still observed well at this distance. Figure 4 shows four intensity distribution plots for the aforementioned distance and different distances to the detector.

In Fig. 4a $z_1 = 0.4$ cm. The image structure somewhat resembles that in Fig. 3c. However, there are differences. First, the structure period is twice as large, which is in complete agreement with the phase contrast theory (i.e., formula (7)), because the magnification factor is $M = 1 + z_1/z_0$. In this case $z_1 = z_0$ and $M = 2$. Second, the beam is a Gaussian with a relatively small width; hence, the contrast is shown on another scale. In fact, only the central period, which corresponds to the Gaussian peak, is minimally distorted.

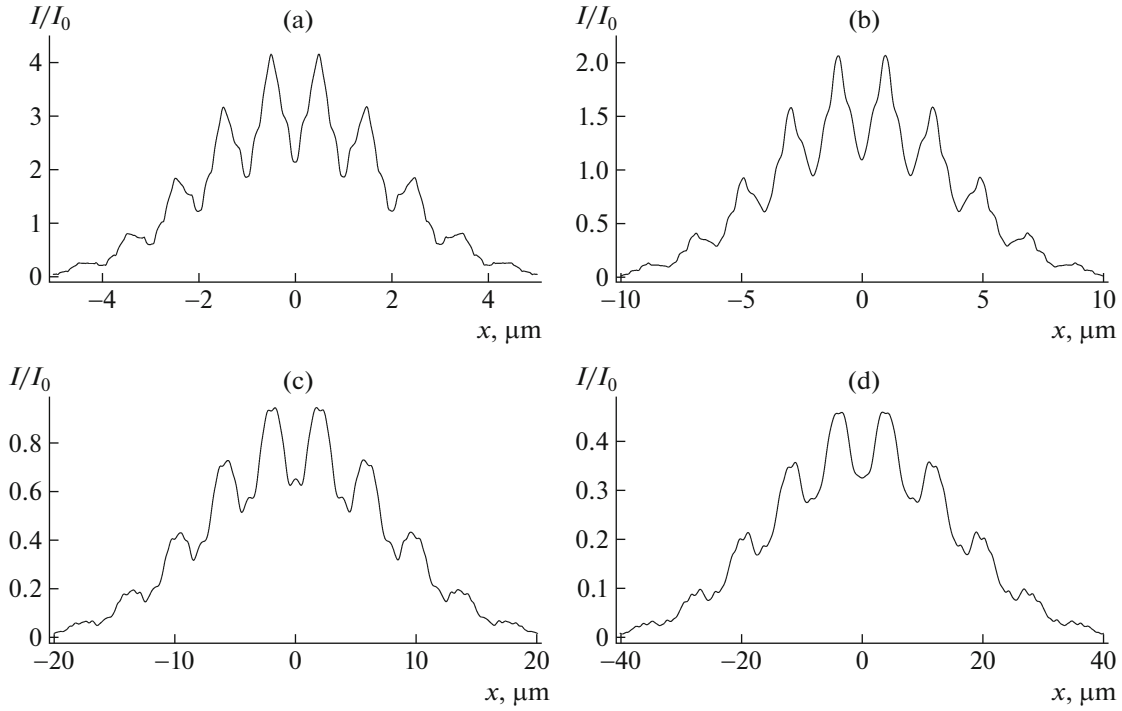

Fig. 4. Phase-contrast images of the photonic crystal at $z_0 = 0.4$ cm and z_1: (a) 0.4, (b) 1.2, (c) 2.8, and (d) 6.0 cm. Intensity I_0 refers to the beginning of CRL.

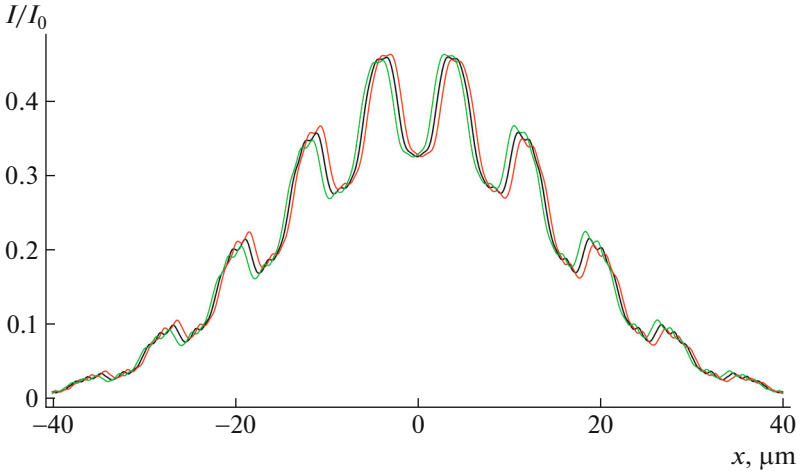

Fig. 5. Phase-contrast images of the photonic crystal at $z_0 = 0.4$ cm, $z_1 = 6.0$ cm, and $x_s = 0$ (middle curve), 50 (right curve), and −50 μm (left curve). The middle curve coincides with the curve in Fig. 4d.

In Fig. 4b $z_1 = 1.2$ cm and $M = 4$. One can see that the image structure changed little, but the period increased by a factor of 4. In Figs. 4c and 4d $z_1 = 2.8$ and 6.0 cm and $M = 8$ and 16, respectively. The structure image continues to change weakly, and, in addition, the contrast slightly decreases. The reason is the finite beam size at the focus. As follows from the theory, for a very small beam size, nothing should change at large distances to the detector. However, these changes are not fundamental, and the photonic crystal period can easily be determined. Moreover, this period is 8 μm in Fig. 4d, and it can easily be measured by a detector with a resolution of 0.5 μm. At the same time, the distance can easily be increased additionally by a factor of 10 or more.

To take into account the influence of the sizes of a real SR source on the photonic crystal image, one must calculate the intensity distribution for all points in the source cross section (with allowance for their brightness) and sum all these images. In Fig. 5 the

intermediate curve corresponds to the plot in Fig. 4d, which was obtained at the point-source transverse coordinate $x_s = 0$. There are also curves for $x_s = 50$ μm (right) and −50 μm (left) in this figure. Note that the curves are not only shifted horizontally but also have slightly different shapes.

The shift can roughly be estimated as follows. It is known from the theory of nanofocusing CRLs [21, 22] that a transverse shift of a point source by a distance $x_s = 50$ μm leads to a shift of its image at the focus by a distance $-M_1x_s$, where the parameter M_1 is calculated by an on-line program [19]. In the case under consideration $M_1 = 6 \times 10^{-4}$. A negative shift of the secondary source leads to a positive shift of the object image with a magnification factor $M_2 = z_1/z_0 = 15$. The total shift is $M_1M_2x_s = 0.45$ μm.

This estimate corresponds on average to the calculation results presented in Fig. 5. However, the curve is not shifted as a whole for the following reason: the beam has a very small transverse size, and different parts of the image correspond to different illuminances of the object, which has a very complex structure. Nevertheless, the curve distortion, being very weak, makes it possible to measure directly the photonic crystal period even on a second-generation SR source. Concerning the third-generation SR sources, they have much smaller sizes, which cannot deteriorate the image at all.

Thus, the following conclusion can be drawn based on the performed computer experiment: the new microscopy scheme, applying the phase-contrast method and nanofocusing CRLs, is able to image structures with a period of 0.5 μm or smaller. Its additional advantage is the high image locality, because the beam has naturally small sizes, which can also be controlled. Moreover, the method is characterized by a high aperture ratio due to the focusing of the initial beam from the SR source. Although the aperture of nanofocusing lenses is small, one can use condensers (i.e., CRLs with a large aperture) and apply cascade focusing.

FUNDING

This study was supported by the Russian Foundation for Basic Research, project no. 19-29-12043mk, in the part concerning the development of the computer program and by the Ministry of Science and Higher Education of the Russian Federation (grant no. 075-15-2021-1362) in the part of carrying out of a computer experiment and analysis of the results.

CONFLICT OF INTEREST

The author declares that he has no conflicts of interest.

REFERENCES

1. A. Snigirev, I. Snigireva, V. Kohn, et al., Rev. Sci. Instrum. **66**, 5486 (1995).
2. A. Snigirev, V. Kohn, I. Snigireva, et al., Nature **384**, 49 (1996).
3. T. S. Argunova and V. G. Kohn, Usp. Fiz. Nauk **189**, 643 (2019). https://doi.org/10.3367/UFNr.2018.06.038371
4. P. A. Prosekov, V. L. Nosik, and A. E. Blagov, Crystallogr. Rep. **66**, 867 (2021).
5. A. Bosak, I. Snigireva, K. S. Napolskii, et al., Adv. Mater. **22**, 3256 (2010). https://doi.org/10.1002/adma.201000173
6. V. G. Kohn and N. V. Tsvigun, Crystallogr. Rep. **59**, 1 (2014).
7. V. Kohn, I. Snigireva, and A. Snigirev, J. Synchrotron Radiat. **21**, 729 (2014). https://doi.org/10.1107/S160057751401056X
8. V. G. Kohn, J. Synchrotron Radiat. **25**, 425 (2018). https://doi.org/10.1107/S1600576717018490
9. C. G. Schroer, M. Kuhlmann, U. T. Hunger, et al., Appl. Phys. Lett. **82**, 1485 (2003). https://doi.org/10.1063/1.1556960
10. C. G. Schroer, O. Kurapova, J. Patommel, et al., Appl. Phys. Lett. **87**, 124103 (2005). https://doi.org/10.1063/1.2053350
11. A. Snigirev, I. Snigireva, V. Kohn, et al., Phys. Rev. Lett. **103**, 064801 (2009). https://doi.org/10.1103/PhysRevLett.103.064801
12. V. G. Kohn, Pis'ma Zh. Eksp. Teor. Fiz. **76**, 701 (2002).
13. V. G. Kohn, Zh. Eksp. Teor. Fiz. **124**, 224 (2003).
14. V. G. Kohn and M. S. Folomeshkin, J. Synchrotron Radiat. **28**, 419 (2021). https://doi.org/10.1107/S1600577520016495
15. V. G. Kohn, J. Synchrotron Radiat. **29**, 615 (2022). https://doi.org/10.1107/S1600577522001345
16. V. G. Kohn and A. Kazimirov, Acta Crystallogr. A **68**, 331 (2012). https://doi.org/10.1107/S0108767312012305
17. V. Kohn, I. Snigireva, and A. Snigirev, Phys. Rev. Lett. **85**, 2745 (2000).
18. http://kohnvict.ucoz.ru/acl/acl.htm
19. http://kohnvict.ucoz.ru/jsp/1-crlpar.htm
20. J. W. Cooley and J. W. Tukey, Math. Comp. **19**, 297 (1965).
21. V. G. Kohn, J. Surface Investigation **3** (3), 358 (2009).
22. V. G. Kohn, J. Synchrotron Radiat. **19**, 84 (2012). https://doi.org/10.1107/S0909049511045778

Translated by Yu. Sin'kov